Available online at www.sciencedirect.com
SCIENCE DIRECT®
Spectrochimica Acta Part A 61 (2005) 2933–2938
SPECTROCHIMICA ACTA PART A
www.elsevier.com/locate/saa

Electrochemical and ESR study of 5-nitrofuryl-containing thiosemicarbazones antiprotozoal drugs

Carolina Rigol[a], C. Olea-Azar[a,*], Fernando Mendizábal[b], Lucía Otero[c], Dinorah Gambino[c], Mercedes González[d], Hugo Cerecetto[d]

[a] *Departamento de Química Inorgánica y Analítica, Facultad de Ciencias Químicas y Farmacéuticas, Universidad de Chile, Olivos 1007 Independencia, Santiago, Chile*
[b] *Departamento de Química, Facultad de Ciencias, Universidad de Chile, Chile*
[c] *Cátedra de Química Inorgánica, DEC, Facultad de Química, Universidad de la República, Uruguay*
[d] *Departamento de Química Orgánica, Facultad de Química/Facultad de Ciencias, Universidad de la República, Uruguay*

Received 6 September 2004; received in revised form 2 November 2004; accepted 2 November 2004

Abstract

Cyclic voltammetry and electron spin resonance (ESR) techniques were used in the investigation of several potential antiprotozoal thiosemicarbazones nitrofurane derivatives.

A self-protonation process involving the protonation of the nitro group due to the presence of an acidic proton in the thiosemicarbazone moiety was observed in the first step of a CEE_{rev} reduction mechanism of these derivatives.

ESR spectra of the free radicals obtained by electrolytic reduction were characterized and analyzed. AM1 methodology was used to obtain the optimized geometries and UB3LYP calculations were performed to obtain the theoretical hyperfine coupling constants. The theoretical study exhibited an unusual assignment of the spin densities showing a free radical centered in the thiosemicarbazone moiety rather than the nitro which are in agreement with the experimental hyperfine pattern.

Keywords: Cyclic voltammetry; ESR; 5-Nitrofurane derivatives; Anion free radical; *T. cruzi*

1. Introduction

5-Nitrofuranes have found popular use in the treatment of parasitic infections because of their antiprotozoal–antibacterial activity [1]. In Latin America, parasitic diseases represent a major health problem. In particular, Chagas' disease (American Trypanosomiasis), caused by the protozoan parasite *Trypanosoma cruzi*, affects approximately 20 million people from Southern California to Argentina and Chile [2,3].

The current chemotherapy against this parasite is still inadequate due to the undesired side effects caused by the drugs in use [4].

Experiments carried out on the main drugs used in Chagas treatment suggest that intracellular reduction followed by redox cycling yielding reactive oxygen species (ROS) may be their major mode of action against *T. cruzi*. These can cause cellular damage directly by reacting with various biological macromolecules, or indirectly by generation of the highly reactive hydroxyl radical via iron-mediated Haber–Weiss and Fenton reactions [5,6,8].

The redox metabolism in trypanosomatids is unique in being based on the bis-glutathionylspermidine conjugate, trypanothione, and the flavoenzyme trypanothione

* Corresponding author. Tel.: +56 2 6782834; fax: +56 2 7370567.
E-mail address: colea@uchile.cl (C. Olea-Azar).

1386-1425/$ – see front matter © 2004 Elsevier B.V. All rights reserved.
doi:10.1016/j.saa.2004.11.003

reductase (TR). The trypanothione system, which replaces the glutathione/glutathione reductase (GR) system, quite omnipresent in mammals, protects the parasites from oxidant damage, among other phenomena. The known sensitivity of trypanosomatids towards ROS renders the enzymes of the trypanothione metabolism promising targets for the development of parasite-specific drugs [7].

We have previously reported studies on antiprotozoal 5-nitrofurfural and 5-nitrothiophene-2-carboxaldehyde derivatives. These compounds showed to generate nitro anion radicals, which were characterized using ESR spectroscopy [8–10].

The study of several drugs designed in order to imitate the trypanothione spermidine group reported the generation of nitro anion and hydroxyl radicals by microsomal reduction in presence of *T. cruzi* epimastigotes [10].

Electron spin resonance (ESR) and electrochemical methods, such as cyclic voltammetry, are now widely accepted and well developed as powerful tools in the identification of paramagnetic intermediates and other reaction products [8,11,12]. On the other hand, density functional methods are capable of providing reasonable predictions for ESR properties, the best results being obtained with the hybrid schemes such as the standard B3LYP [13].

In the present work, a family of eight 5-nitrofuryl-containing thiosemicarbazone derivatives were studied [14]. These compounds were developed as hybrid compounds that could act against *T. cruzi* by a dual mechanism of action, oxidative stress and inhibition of cruzain throughout their nitro and thiosemicarbazone moieties, respectively. Cruzain is the major cysteine protease of *T. cruzi*; cruzain inhibition is currently one of the most advanced and widely studied strategies in the design of new drugs for the treatment of American trypanosomiasis [15]. Recently, it has described that some thiosemicarbazone derivatives exhibit potent activity against cruzain as well as trypanocidal activity against parasites in cell culture [16]. The reduction pathway of this family of compounds was studied using cyclic voltammetry and the radical species were characterized using ESR. In order to estimate the theoretical hyperfine splitting constants, an open shell B3LYP methodology was carried out.

2. Experimental section and theoretical methods

2.1. Samples

The 5-nitrofuryl-containing thiosemicarbazone derivatives (Fig. 1) were synthesized according to methods described earlier [14].

2.2. Cyclic voltammetry

DMSO (spectroscopy grade) was obtained from Aldrich. Tetrabuthylammonium perchlorate (TBAP), used as supporting electrolyte, was obtained from Fluka. Cyclic voltammetry was carried out using a Metrohm 693 VA instrument with a 694 VA Stand convertor and a 693 VA Processor, in DMSO (ca. 1.0×10^{-3} mol L^{-1}), under a nitrogen atmosphere at room temperature, with TBAP (ca. 0.1 mol L^{-1}), using a three-electrode cell. A mercury-dropping electrode was used as the working electrode, a platinum wire as the auxiliary electrode, and saturated calomel as the reference electrode.

2.3. ESR spectroscopy

ESR spectra were recorded in the X band (9.7 GHz) using a Bruker ECS 106 spectrometer with a rectangular cavity and 50 kHz field modulation. The nitro radicals were generated by electrolytic reduction in situ under the same conditions of temperature, atmosphere and concentrations stated at the voltammetric experiment. Simulations of the spectra were made using the Simfonia Version 1.25 software. The hyperfine splitting constants were estimated to be accurate within 0.05 G.

2.4. Theoretical calculations

Full geometry optimizations, in vacuo, of the nitrofuranes in spin-paired forms were carried out using AM1 semi empirical methodology. The theoretical hyperfine constants were calculated using the open shell UB3LYP methodology with the 6-31G* basis set.

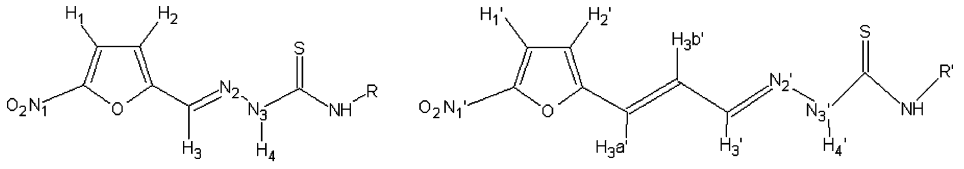

NS1 R = Et
NS3 R = Ph
NS5 R = Me
NS7 R = H

NS2 R = Et
NS4 R = Ph
NS6 R = Me
NS8 R = H

Fig. 1. Chemical structure of the nitrofuran of thiosemicarbazone derivatives.

3. Results and discussion

3.1. Cyclic voltammetry

Fig. 2 shows the voltammogram displayed by the nitrofurane family when a DMSO solution of 1 mM of nitrofurane NS3 derivative and 100 mM of TBAP is swept from 0 to −2.6 V. We notice clearly a one-electron reversible transfer (peak IIIc/IIIa Fig. 2) corresponding to the generation of the radical anion $RNO_2^{\bullet -}$ around −0.80 V. We studied the stability of the radical intermediates by changing the electrochemical conditions i.e. the scan rate, while keeping the chemical conditions of the solution unaltered. We observe that the ip_a/ip_c ratio calculated with the Nicholson and Shain equation [17] increases slightly as the scan rate increases (from 100 to 2000 mV/s), as is typical for a reversible charge transfer (results not shown) [18]. All of the nitrofuranes exhibited lower $E_{1/2}$ ($E_{1/2} = (E_a + E_c)/2$) values than Nifurtimox (−0.88 V [8]) showing a higher capacity to be reduced, hence, a better ability to generate the radical species.

Table 1 lists the values of voltammetric peaks and the anodic and cathodic currents for all compounds plus nifurtimox taken from reference [8]. All compounds display comparable voltammetric behaviour, in DMSO.

The subsequent more negative three-electron irreversible cathodic peak (IVc, Fig. 2) belonging to the production of the hydroxylamine derivative [10] is irreversible in the whole range of sweep rates used (100–2000 mV/s) for all eight compounds. Sharp peaks can be noticed in some voltammograms at low sweep rates as a result of an adsorption phenomenon in the electrode surface due to the presence in the molecules of the thiocarbonyl group (results not shown).

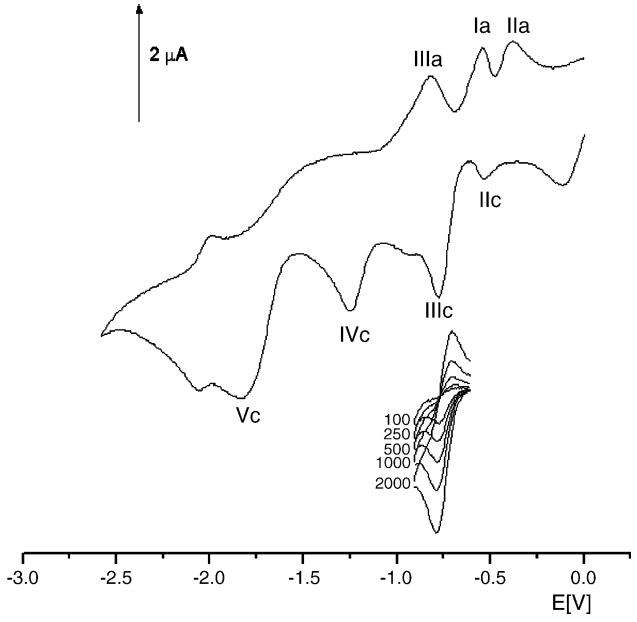

Fig. 2. Cyclic voltammograms of 1 mM NS3 sweep rates of wave III from 100 to 2000 in 100% DMSO with 0.1 M TBAP.

Table 1
Cyclic voltammetric parameters corresponding to the nitro moiety reduction of couple III and IV vs. saturated calomel electrode in DMSO

Nitrofurans	E_{pIIIc} (V)	E_{pIIIa} (V)	ΔE (V)	$E_{1/2}$ (V)[a]	ip_a/ip_c	E_{pIVc} (V)
NS1	−0.79	−0.71	0.08	−0.75	1.03	−1.42
NS2	−0.79	−0.71	0.08	−0.75	1.07	−1.28
NS3	−0.78	−0.70	0.08	−0.74	0.88	−1.26
NS4	−0.77	−0.70	0.07	−0.74	0.94	−1.12
NS5	−0.79	−0.71	0.08	−0.75	1.04	−1.40
NS6	−0.79	−0.70	0.09	−0.75	1.08	−1.26
NS7	−0.84	−0.75	0.09	−0.80	0.95	−1.42
NS8	−0.84	−0.72	0.12	−0.78	1.03	−1.31
Nifurtimox	−0.91[b]	−0.85	0.06	−0.88	1.01	–[c]

[a] $E_{1/2} = (E_{pIIIc} + E_{pIIIa})/2$.
[b] Data from reference [8].
[c] Data not shown in reference [8].

The voltammogram of all nitrofuranes show one anodic peak around −0.6 V (Ia), that could be attributed to the reoxidation process of the hydroxylamine RNHOH generated in IVc into RNO. A successive second sweep exhibits a shoulder peak near IIc which could be attributed to the cathodic counterpart from the reversible reaction RNHOH ⇆ RNO + $2e^-$ + $2H^+$ (figure not shown). In addition, a prepeak (IIc) appears even before the reduction of the nitro group, meaning that the nitro group follows another reaction path beside the known electron-transfer mechanism of nitroaromatic compounds in aprotic media. This prepeak corresponds to the four-electron reduction of a small portion of the molecules reaching the electrode surface, while the remaining portion supplies the protons required for this reduction. The presence of the nitro group increases the acidity of the N–H moiety from the thiosemicarbazone group (N_3–H_4, Fig. 1) which becomes capable of protonating the nitro group of a minor part of molecules in the solution, resulting into a lower intensity of these signals. This is a typical behavior of a self-protonation phenomenon displayed by nitrocompounds with acidic moieties in their structure [19–22]. Peak IIa as the counterpart of IIc belongs actually to the two-electron oxidation of the hydroxylamine into the nitroso compound as happens in Ia. In summary, we observe, thus in waves III and IV, the reduction of the anionic molecules that supplied the protons for reaction Ic to take place.

Peak V observed in the voltammograms is presumed to belong to the reduction of the imine moiety (CH=N) of the thiosemicarbazone group [23]. Peaks not labeled in Fig. 2 correspond to the reduction of the support electrolyte (TBAP).

Finally, the reduction mechanism for these nitrofurane derivatives comprising waves III–V, and prepeaks I and II observed in the cyclic voltammograms (Fig. 2), is proposed in Fig. 3.

3.2. Electron spin resonance and theoretical calculations

The nitrofurane free radicals characterized by ESR were prepared in situ by electrochemical reductions in DMSO,

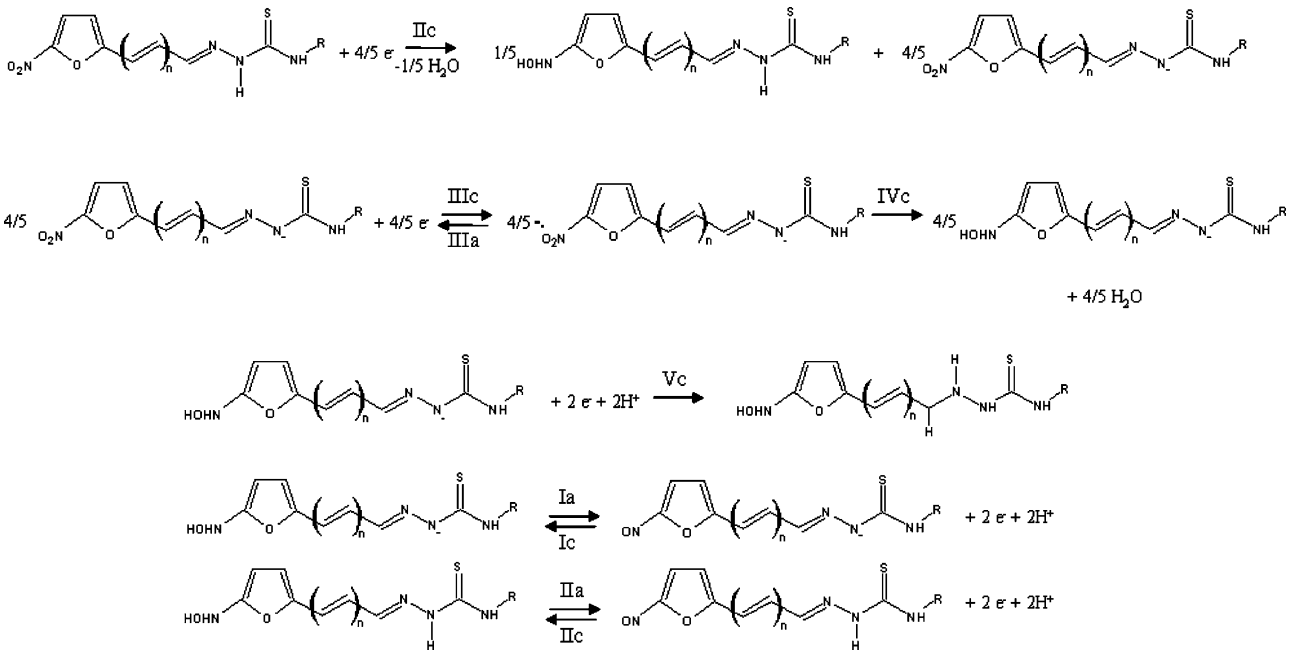

Fig. 3. Reduction mechanism suggested for the nitrofurane derivatives.

applying a potential corresponding to peak IIIc obtained from the voltammetric experiments. All the investigated structures formed stable paramagnetic intermediates at that first reduction step.

The interpretation of the ESR by means of a simulation process confirmed the stabilities of these radical species due to the delocalization of the unpaired electron. The simulation of the spectra was made using hyperfine coupling constants (hfccs) obtained from the DFT calculations, modifying the linewidth, modulation amplitude and Lorentzian/Gaussian component until the obtained spectra reached the greatest similarity with the experimental ones. Table 2 reports the hfccs obtained from the DFT calculations.

NS1 free radical (Fig. 1) displays a simulated spectrum of two triplets assigned to the nitro group (N_1, Fig. 1) and the imine (N_2) nitrogen atoms and four doublets assigned to nuclei H_1 from the furan ring, H_3 belonging to the imine group, and two of the hydrogen atoms of the CH_2 moiety of the ethyl group which are assigned by theoretical calculation.

The simulated spectrum of NS3 radical results from a pattern of three triplets from nitrogens N_1, N_2 and N_3 directly bound to N_2, and two doublets from H_1 and H_3.

NS5 free radical spectrum was simulated in terms of two triplets assigned to nuclei N_1 and N_2 and three doublets assigned, one to nuclei H_1, and the others to two of the hydrogen atoms of the methyl group.

NS7 free radical spectrum was simulated in terms of three triplets from nitrogens N_1, N_2 and N_3 and four doublets belonging to hydrogens H_1, H_3 and both hydrogens of the amine moiety.

In the analysis of NS2 free radical spectrum, we observe a signal pattern of three triplets assigned to the nitrogen of the nitro group (N_1'), the imine (N_2') and the thiosemicarbazone (N_3'), and four doublets assigned to nuclei H_1' and H_2' from the furan ring and H_3a' and H_3b' belonging to the CH=CH group.

Table 2
Hyperfine splittings (Gauss) assigned by UB3LYP/6-31G* methodology and experimental *g* values nitro anion radicals

Nitrofuran	aN_1	aN_2	aN_3	aH_1	aH_3	aR	*g* values
NS1	2.49	8.76	–	3.43	1.33	2 × 0.36 (CH_2)	2.0170
NS3	2.07	5.47	1.09	2.66	1.50	–	2.0164
NS5	2.16	7.43	–	3.02	–	2 × 2.18 (CH_3)	2.0162
NS7	1.19	6.98	1.57	1.17	2.59	2 × 1.06 (NH_2)	2.0158

Nitrofuran	aN_1'	aN_2'	aN_3'	aH_1'	aH_2'	aH_3a'	aH_3b'	aH_3'	aR′	*g* values
NS2	0.99	6.54	1.20	0.68	1.32	3.08	6.52	–	–	2.0167
NS4	0.78	4.42	1.20	–	1.25	2.71	3.94	0.73	–	2.0177
NS6	1.54	6.24	1.57	1.08	1.08	4.82	4.84	0.94	1.28 (CH_3)	2.0156
NS8	0.99	6.49	1.14	0.68	1.30	3.04	6.55	–	–	2.0158

The magnetic nuclei are named according to Fig. 1.

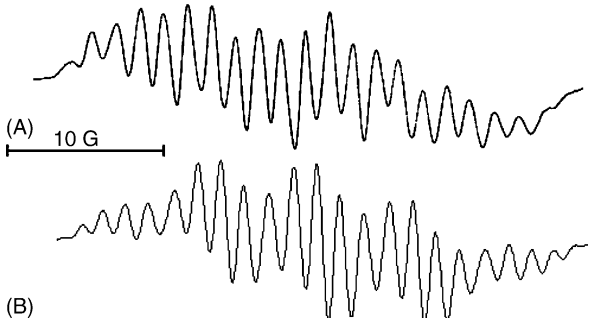

Fig. 4. (A) ESR experimental spectrum of NS6 nitro radical produced by an electrochemical generation in DMSO with 1 mM of nitrofurane and 100 mM TBAP. *Spectrometer conditions*: microwave frequency, 9.71 GHz; microwave power, 20 mW; modulation amplitude, 0.2 G; scan rate, 1.25 G/s; time constant, 0.5 s; number of scans 15. (B) Computer simulation of the same spectrum using DFT-calculated hfccs. Spectrum was simulated using the following parameters: line width, 0.9 G; ratio Lorentzian/Gaussian, 1.0; hyperfine constants included in Table 2. G, Gauss.

NS4 free radical spectrum was simulated in terms three triplets from nitrogens N'_1, N'_2 and N'_3 and four doublets from H'_2, H_3a', H_3b' and H'_3.

The simulated spectrum of NS6 radical form (Fig. 4) resulted from a signal pattern of three triplets assigned to nuclei N'_1, N'_2 and N'_3, and six doublets assigned to nuclei H'_1, H'_2, H_3a', H_3b', H'_3, and one hydrogen atom of the methyl group.

Finally, NS8 free radical spectrum was simulated in terms of three triplets from nitrogens N'_1, N'_2 and N'_3 and four doublets belonging to hydrogens H'_1, H'_2, H_3a', and H_3b'.

Concerning the analysis of the data obtained from the theoretical calculations and its use in the simulation of the ESR spectra, we found that the optimization of the geometries showed a direct dependence of the structure's conformation on the hfccs. Nitrocompounds typically localize their unpaired electron in the nitro group [6], however, this family of nitrofuranes showed a different behavior centering the spin electron density around nuclei N_2, N'_2 and H_3, H_3a', H_3b' (Fig. 1). The radical species of NS1, NS3, NS5, NS7 (Fig. 1) display delocalized spin densities between nuclei N_1 (nitro group), H_1, N_2 and H_3 (Table 2). On the other hand, radicals of NS2, NS4, NS6, NS8 delocalize the unpaired electron through the conjugate planar system providing nuclei N'_2, H_3a' and H_3b' with high spin densities.

4. Concluding remarks

All nitrofuranes studied showed lower $E_{1/2}$ potentials than Chagas' treatment drug Nifurtimox which provides them of promissory antitrypanosomal activity. The reduction of the nitro group of the thiosemicarbazone nitrofuranes exhibits a self-protonation reaction between the acidic proton of the thiosemicarbazone group (H_4, H'_4, Fig. 1) and the nitro moiety revealing a CEE_{rev} reduction mechanism. This kind of self-protonating reactions destabilizes the nitro radical anion-giving place to a multi-electron reduction of the nitro moiety to produce the corresponding anion hydroxylamine intermediate [19].

The donor/acceptor capacity of the substituents does not seem to affect significantly the reduction potentials of the derivatives; only the non-substituted derivatives display differences in their potentials. However, the conformations adopted by the radical species, influenced by their interaction with the solvent, affects in the delocalization of the unpaired electron.

The theoretical calculations showed that the spin density is in general higher in the thiosemicarbazone nitrogen, opposing to the results of other nitro radical species [7], which means that the unpaired electron accepted by the nitro moiety, as stated by the voltammetric study, rapidly delocalizes to the other nuclei of the molecule.

UB3LYP/6-31G* proved to be a good methodology in the calculation of ESR hyperfine coupling constants for this kind of molecules, making the simulation process much simpler.

Acknowledgments

This research was supported by FONDECYT 1030949 grant, CONICYT AT-4040020 grant, U. de Chile DID graduate grant PG-65, CEPEDEQ, RELAQ, and TWAS. L.O. thanks to UDELAR and RTPD for training fellowships.

References

[1] W.Z. Raether, H. Hanel, Parasitol. Res. 1 (2003) 19.
[2] J.A. Urbina, R. Docampo, Trends Parasitol. 19 (2003) 495.
[3] World Health Organization, http://www.who.int/ctd/chagas/burdens.htm.
[4] H. Cerecetto, M. Gonzalez, Curr. Top. Med. Chem. 2 (2002) 1187.
[5] R. Docampo, S.N.J. Moreno, Rev. Infect. Dis. 6 (1984) 223.
[6] S.N. Moreno, R.P. Mason, R. Docampo, J. Biol. Chem. 259 (1984) 6298.
[7] L. Thomson, A. Denicola, R. Radi, Arch. Biochem. Biophys. 412 (2003) 55.
[8] C. Olea-Azar, A.M. Atria, F. Mendizabal, R. Di Maio, G. Seoane, H. Cerecetto, Spectrosc. Lett. 31 (1998) 99.
[9] C. Olea-Azar, A. Atria, R. Di Maio, G. Seoane, H. Cerecetto, Spectrosc. Lett. 31 (1998) 849.
[10] C. Olea-Azar, C. Rigol, F. Mendizabal, A. Morello, J.D. Maya, C. Moncada, E. Cabrera, R. Di Maio, M. Gonzalez, H. Cerecetto, Free Radic. Res. 37 (2003) 993.
[11] C. Olea-Azar, C. Rigol, F. Mendizabal, H. Cerecetto, R. Di Maio, M. González, W. Porcal, C. Moncada, A. Morello, Y. Repetto, J.D. Maya, Spectrochim. Acta A 59 (2003) 69.
[12] J. Wang, Analytical Electrochemistry, second ed., Wiley-VCH, 2000, p. 28.
[13] W. Koch, M.C. Holthausen, A Chemist's Guide to Density Functional Theory, second ed., Wiley-VCH Verlag GMBH, 2001 (Chapter 11).
[14] G. Aguirre, L. Boiani, H. Cerecetto, M. Fernández, M. González, A. Denicola, L. Otero, D. Gambino, C. Rigol, C. Olea-Azar, M. Faúndez, Med. Chem. 12 (2004) 4885.
[15] (a) J.J. Cazzulo, Curr. Top. Med. Chem. 2 (2002) 1261;
(b) L. Huang, A. Lee, J.A. Ellman, J. Med. Chem. 45 (2002) 676.

[16] (a) X. Du, E. Hansell, J.C. Engel, C.R. Carey, F.E. Cohen, J.H. Mc Kerrow, Chem. Biol. 7 (2000) 733;
(b) X. Du, C. Guo, E. Hansell, P.S. Doyle, C.R. Carey, T.P. Holler, J.H. McKerrow, F.E. Cohen, J. Med. Chem. 45 (2002) 2695.
[17] R.S. Nicholson, Anal. Chem. 38 (1966) 1406.
[18] R. Nicholson, I. Shain, Anal. Chem. 36 (1964) 706.
[19] J.A. Bautista-Martínez, I. González, M. Aguilar-Martínez, Electrochim. Acta 49 (2004) 3403.
[20] J. Carbajo, S. Bollo, L.J. Núñez-Vergara, A. Campero, J.A. Squella, J. Electroanal. Chem. 531 (2002) 187.
[21] G. Kokkinidis, A. Kelaidopoulou, J. Electroanal. Chem. 414 (1996) 197.
[22] C. Amatore, G. Capobianco, G. Farnia, G. Sandonà, J.M. Savéant, M.G. Severin, E. Vianello, J. Am. Chem. Soc. 107 (1985) 1815.
[23] S. Bollo, E. Soto-Bustamante, L.J. Núñez-Vergara, J.A. Squella, J. Electroanal. Chem. 492 (2000) 54.